polymers

MDPI

Article

Stretchable, Adhesive, and Biocompatible Hydrogel Based on Iron–Dopamine Complexes

Celine Lee [1], He-Shin Huang [1], Yun-Ying Wang [1], You-Sheng Zhang [1], Rajan Deepan Chakravarthy [2], Mei-Yu Yeh [1,*], Hsin-Chieh Lin [2,*] and Jeng Wei [3,*]

[1] Department of Chemistry, Chung Yuan Christian University, No. 200, Zhongbei Rd., Zhongli Dist., Taoyuan City 320314, Taiwan; clys0813@gmail.com (C.L.); candyhuang16@gmail.com (H.-S.H.); g11063013@cycu.org.tw (Y.-Y.W.); brian20010418@gmail.com (Y.-S.Z.)

[2] Department of Materials Science and Engineering, National Yang Ming Chiao Tung University, No. 1001, Daxue Rd., East Dist., Hsinchu City 300093, Taiwan; rdciitmadras@gmail.com

[3] Heart Center, Cheng Hsin General Hospital, No. 45, Cheng Hsin St., Beitou Dist., Taipei City 112401, Taiwan

* Correspondence: myyeh@cycu.edu.tw (M.-Y.Y.); hclin45@nycu.edu.tw (H.-C.L.); jengwei@mac.com (J.W.)

Abstract: Hydrogels' exceptional mechanical strength and skin-adhesion characteristics offer significant advantages for various applications, particularly in the fields of tissue adhesion and wearable sensors. Herein, we incorporated a combination of metal-coordination and hydrogen-bonding forces in the design of stretchable and adhesive hydrogels. We synthesized four hydrogels, namely PAID-0, PAID-1, PAID-2, and PAID-3, consisting of acrylamide (AAM), *N*,*N*′-methylene-bis-acrylamide (MBA), and methacrylic-modified dopamine (DA). The impact of different ratios of iron (III) ions to DA on each hydrogel's performance was investigated. Our results demonstrate that the incorporation of iron–dopamine complexes significantly enhances the mechanical strength of the hydrogel. Interestingly, as the DA content increased, we observed a continuous and substantial improvement in both the stretchability and skin adhesiveness of the hydrogel. Among the hydrogels tested, PAID-3, which exhibited optimal mechanical properties, was selected for adhesion testing on various materials. Impressively, PAID-3 demonstrated excellent adhesion to diverse materials and, combined with the low cytotoxicity of PAID hydrogel, holds great promise as an innovative option for biomedical engineering applications.

Keywords: stretchable; adhesive; hydrogel; polyacrylamide; dopamine

check for updates

Citation: Lee, C.; Huang, H.-S.; Wang, Y.-Y.; Zhang, Y.-S.; Chakravarthy, R.D.; Yeh, M.-Y.; Lin, H.-C.; Wei, J. Stretchable, Adhesive, and Biocompatible Hydrogel Based on Iron–Dopamine Complexes. *Polymers* **2023**, *15*, 4378. https://doi.org/10.3390/polym15224378

Academic Editors: Dermot Brougham, Daniel Hermida-Merino and Bing Wu

Received: 31 August 2023
Revised: 15 October 2023
Accepted: 31 October 2023
Published: 10 November 2023

Copyright: © 2023 by the authors. Licensee MDPI, Basel, Switzerland. This article is an open access article distributed under the terms and conditions of the Creative Commons Attribution (CC BY) license (https://creativecommons.org/licenses/by/4.0/).

1. Introduction

Hydrogels, recognized as soft materials in the field of materials science, are three-dimensional (3D) cross-linked polymer networks with the remarkable capability of absorbing and retaining a substantial amount of water [1–7]. The significant attention hydrogels have received is due to their high water content and the related potential they hold for numerous biomedical applications, including tissue engineering [8–12], soft robotics [13–17], wearable devices [18–21], personal care [22–24], and more. Hydrogels are commonly prepared using both synthetic and natural polymers. Synthetic hydrogels employ diverse chemistries to cross-link synthetic polymer molecules, resulting in hydrogels that exhibit relatively high mechanical strength. However, once these hydrogels are formed, they become challenging to remold. Consequently, they are not suitable for many applications, particularly in the fields of cell culture and tissue engineering. To address this limitation, the incorporation of physical non-covalent bond forces, such as metal coordination, host-guest interactions, ionic interactions, hydrogen bonding, hydrophobic interactions, and π-π interactions, is employed to enhance the flexibility, adjustability, and reversibility of hydrogels [25–31].

Inspired by nature, specific biomaterials that possess abundant metal-coordination bonds, for example, mussels, exhibit an impressive blend of high toughness, adhesion,

and reversibility [32–37]. As a result, this concept of biomaterials is extensively used by researchers in the development of functional hydrogels [38–44]. Das et al. have developed hydrogels of poly(methacrylamide-*co*-vinylimidazole)-M^{2+} (M = Ni and Zn), which demonstrate an exceptionally broad range of mechanical properties, rapid self-recovery, remarkable fatigue resistance, efficient self-healing, and temperature-dependent shape memory behavior [38]. Hao et al. have devised metal-ligand-coordinated hydrogels with adjustable strength and thermosensitivity [39]. Wu and Zheng have reported a physical hydrogel comprised of poly(acrylamide-*co*-acrylic acid) (P(AAm-*co*-AAc)) cross-linked by carboxyl–Fe^{3+} coordination complexes. This hydrogel exhibits remarkable stiffness, toughness, fatigue resistance, and the ability to undergo stimulation-triggered healing [42]. More recently, Wu et al. have created robust hydrazide-transition metal-coordination complexes to enhance the toughness of hydrogels [43].

Therefore, in this study, we chose to employ the approach of metal coordination to improve the mechanical properties of hydrogels. We specifically opted to utilize dopamine as a building block due to its reputation for forming iron–dopamine complexes [33,44]. Simultaneously, dopamine has the potential to engage in aromatic π-stack interactions with drugs like bortezomib, doxorubicin, topotecan, and others, facilitating controlled drug delivery for cancer treatment [45–47]. Furthermore, dopamine holds promise for emulating mussel adhesives, offering excellent adhesion properties. We synthesized four hydrogels, namely PAID-0, PAID-1, PAID-2, and PAID-3, composed of acrylamide (AAM), *N*,*N*′-methylene-bis-acrylamide (MBA), and methacrylic-modified dopamine (DA). Our investigation focused on evaluating the impact of two factors: (1) the presence of iron–dopamine complexes (PAID-0 served as the control); and (2) the influence of hydrogen-bonding interactions involving dopamine on the mechanical and adhesive properties of the hydrogels. We demonstrated that the incorporation of iron–dopamine complexes substantially enhances the mechanical strength of the hydrogel. Notably, with increasing dopamine content, we observed a continuous and pronounced improvement in both the stretchability and skin-adhesion properties of the hydrogel. This discovery opens up new possibilities for the application of tissue adhesion and wearable sensors.

2. Materials and Methods

2.1. Materials

Acrylamide and 3-hydroxytyramine (dopamine) hydrochloride were obtained from Acros Organics (Geel, Antwerp, Belgium); iron (III) chloride hexahydrate and *N*,*N*′-methylenebisacrylamide were sourced from Alfa Aesar (Ward Hill, MA, USA). The compound 2-hydroxy-4′-(2-hydroxyethoxy)-2-methylpropiophenone (Irgacure 2959) was acquired from Sigma-Aldrich (St. Louis, MO, USA). Methacrylic-modified dopamine was synthesized following the protocol outlined in the literature (for further details, refer to the Supporting Information) [48]. Deionized water was utilized in all experiments.

2.2. Preparation of Hydrogels

PAID hydrogels were synthesized through the radical polymerization of acrylamide, iron (III) chloride hexahydrate, and methacrylic-modified dopamine in the presence of *N*,*N*′-methylenebisacrylamide as a cross-linker and Irgacure 2959 (2 mol % to monomer) as a radical initiator in deionized water. The specific compositions of the hydrogels were listed in Table S1 (see Supplementary Materials).

2.3. Characterizations

Nuclear magnetic resonance (NMR) spectra were obtained using a Bruker (Billerica, MA, USA) AVANCEII-400 MHz spectrometer, with D_2O serving as the solvent. The molecular characteristics and interactions of PAID hydrogels were assessed using a Thermo Fisher Scientific (Waltham, MA, USA) Nicolet iS5 Fourier transform infrared (FT-IR) spectrometer, while the morphologies of the hydrogels were examined through scanning electron microscopy (SEM) using the JEOL (Tokyo, Japan) JSM-7600F model. To prepare the test

samples, the hydrogels were subjected to freeze-vacuum drying. Briefly, the hydrogel samples were rapidly frozen in liquid nitrogen and subsequently lyophilized using a freeze-dryer system under vacuum conditions at a temperature of −80 °C for a minimum of 24 h, allowing all the water to sublimate.

2.4. Mechanical Measurements

The PAID hydrogels underwent tensile testing using a Gotech (Taichung, Taiwan) AI-3000-U tensile tester. Rheological measurements were conducted using a TA rheometer (DHR-1, New Castle, Delaware, USA) equipped with a parallel plate setup. The setup consisted of a 20-millimeter-diameter plate with a 1 mm gap between them. Dynamic oscillatory frequency sweep experiments were performed to determine the shear storage modulus (G′) and loss modulus (G′′) as a function of angular frequency (ω). The measurements were taken across the range of ω from 0.1 to 100 rad/sec at a strain (γ) of 1% and at a temperature of 25 °C.

2.5. Biocompatibility of Hydrogels

The biocompatibility of PAID hydrogels was assessed by cultivating L929 cells with an extraction medium. To prepare the extraction medium, PAID-0, PAID-1, and PAID-3 hydrogels were immersed in Dulbecco's Modified Eagle Medium (DMEM, Gibco, Life Technologies, Carlsbad, CA, USA) at a volume ratio of 1:10 (hydrogel volume to medium volume) and incubated at 37 °C for two days. L929 cells were seeded in 96-well plates and cultured with DMEM at 37 °C under 5% CO_2 for one day. Subsequently, the DMEM was replaced with the extraction medium, allowing the cells to grow for one, three, and seven days. Cell viability assays were performed on the L929 cells cultured with the extraction medium and DMEM using the MTT reagent. The resulting solution's optical density was measured at 595 nm using a BioTek (Winooski, VT, USA) 800 TS microplate reader. Cells that were not exposed to the test hydrogels were designated as the control group.

3. Results and Discussion

3.1. Preparation of PAID Hydrogels

Scheme 1 presents the schematic diagram of the PAID hydrogels. We utilized AAM, MBA, and different ratios of iron (III) ions to DA to prepare the hydrogels, namely PAID-1 (iron ion: DA = 1:3), PAID-2 (iron ion: DA = 1:6), and PAID-3 (iron ion: DA = 1:9); however, continuously increasing the ratio of DA will deteriorate the formability of the hydrogel, resulting in a sticky or pasty consistency. Meanwhile, we also prepared PAID-0 (iron ion: DA = 0:3) for comparison with PAID-1 in order to understand the influence of iron ions on the hydrogel. As shown in Figure 1, the appearance of PAID-0 is a transparent white hydrogel, and, upon the addition of $FeCl_3 \cdot 6H_2O$, the hydrogels transform into transparent light yellow hydrogels (PAID-1, PAID-2, and PAID-3). These indications suggest that the addition of iron ions may lead to the formation of an iron–DA complex, resulting in a significant change in the appearance of the hydrogel.

3.2. Spectral Analysis and Morphologies of PAID Hydrogels

We employ Fourier transform infrared spectroscopy (FT-IR) to analyze PAID hydrogels and investigate the intermolecular forces between iron ions and polymers (DA components). Through the analysis of the absorbance FT-IR peaks of PAID-0, it was observed that the absorption bands at 3375 and 3208 cm^{-1} were indicative of the N–H and/or O–H stretching vibration [49]. Additionally, the absorption bands around 1665 and 1435 cm^{-1} were characteristic of C=O stretching in the amide group and C=C stretching in aromatics, respectively [50,51]. It is worth noting that the O–H stretching bands manifest at lower frequencies, i.e., 3343 and 3198 cm^{-1}, suggesting the potential formation of iron–DA complexes in PAID-1, PAID-2, and PAID-3 (Figure 2) [52]. In the meantime, the C=O and C=C (aromatic) signals likewise shift to lower wavenumbers with an increasing DA content, indicating that the elevated DA content might enhance hydrogen-bonding and

π-π-stacking interactions [53]. Moreover, we conducted a comparison between the PAID-0 hydrogel and the AAM/MBA hydrogel described in the literature [54,55]. Our observations revealed that, in contrast to the AAM/MBA hydrogel, the N-H and C=O vibrations in the PAID-0 gel shifted towards lower wavenumbers, possibly due to the enhanced hydrogen bonds resulting from the incorporation of DA. Based on the FT-IR data, we have discerned plausible molecular interactions within PAID hydrogels, involving metal-coordination, hydrogen-bonding, and π-π-stacking interactions (Figure 3). Subsequently, we used a scanning electron microscope (SEM) to examine the nanostructures of the PAID hydrogels. As can be seen in Figure 4, PAID-0 showed a uniform and flat structure, whereas PAID-1, PAID-2, and PAID-3 exhibited distinct layered structures. This observation suggests that the presence of iron ions can possibly trigger the formation of iron–DA complexes. Moreover, as the amount of DA increases, the layered structure becomes more densely packed, implying that the stretchability of the hydrogel can be enhanced as a result. The SEM analysis revealing layered structures in PAID-1, PAID-2, and PAID-3 further strengthens the evidence of the intermolecular forces present in their FT-IR spectra.

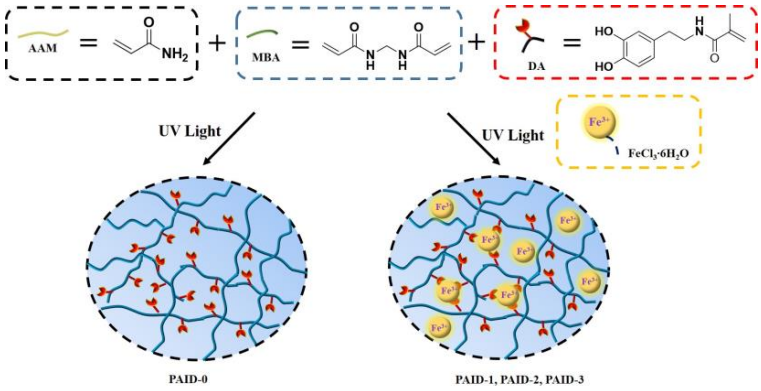

Scheme 1. Schematic diagram of PAID hydrogel, where acrylamide is AAM, *N,N′*-methylene-bis-acrylamide is MBA, and methacrylic-modified dopamine is DA.

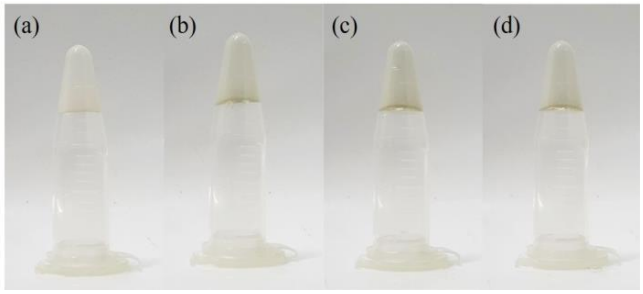

Figure 1. Photographs of (**a**) PAID-0, (**b**) PAID-1, (**c**) PAID-2, and (**d**) PAID-3 hydrogels.

3.3. Mechanical Properties of PAID Hydrogels

It is known that tensile stress-strain analysis and rheology play crucial roles in various fields of science and engineering. On the one hand, tensile stress-strain analysis helps in designing and assessing the mechanical performance of materials, determining their suitability for specific applications [56,57]. On the other hand, rheology finds widespread applications across diverse fields, including polymer processing, chemical engineering, and pharmaceuticals. The importance of rheology lies in understanding the flow and deformation behavior of materials, which is critical for optimizing processes and developing high-quality products [58,59]. In Figure 5, the tensile stress-strain curves of PAID hydrogels are presented. It was found that PAID-0 exhibited a tensile strength of 4.7 kPa and an elongation break of 675%. Upon the introduction of iron ions into PAID-0, i.e., PAID-1, both the tensile strength and elongation break increased to 12.6 kPa and 743%, respectively.

The dramatic enhancement in tensile strength of PAID-1 compared to PAID-0 is likely attributed to the formation of a tris-complex between iron and DA [44]. By keeping the amount of iron ions constant and progressively increasing the amount of DA, we observed a continuous increase in elongation at break; however, there was a decrease in tensile strength. Specifically, for PAID-2 and PAID-3, the tensile strength values were reduced to 10.7 kPa and 8.0 kPa, respectively, while the corresponding elongation break values were measured at 882% and 1011%. The elevated elongation break values in PAID-2 and PAID-3 are probably due to the formation of additional reversible noncovalent bonds, such as hydrogen bonding and/or π-π interactions, ultimately resulting in the enhanced stretchability of the hydrogel. This improvement in mechanical properties aligns with the findings derived from the SEM images presented in Figure 4. The SEM images provided visual evidence that the microstructure of PAID-3 supports higher elongation before failure, which is consistent with the increased elongation break values observed in the mechanical testing. Furthermore, when compared to the metal coordination hydrogels reported in the literature, PAID-3 presented outstanding stretchability, reaching 1011% strain, as indicated in Table S2. This remarkable stretchability opens up possibilities for various applications, particularly in scenarios where a hydrogel with high mechanical flexibility is required, such as in biomedical devices and tissue engineering. These findings highlight the potential of PAID hydrogels to provide innovative solutions in materials science and biotechnology. Figure 6 displays the dynamic rheological behaviors of PAID hydrogels: all of them exhibited a storage modulus (G′) higher than the loss modulus (G″), indicating their viscoelastic solid nature. The values of G′ were determined to be 251 Pa for PAID-0, 1390 Pa for PAID-1, 699 Pa for PAID-2, and 352 Pa for PAID-3. All these hydrogels show G′ values exceeding 100 Pa, which provides sufficient support for cell culture by being able to bear the weight of cells [60].

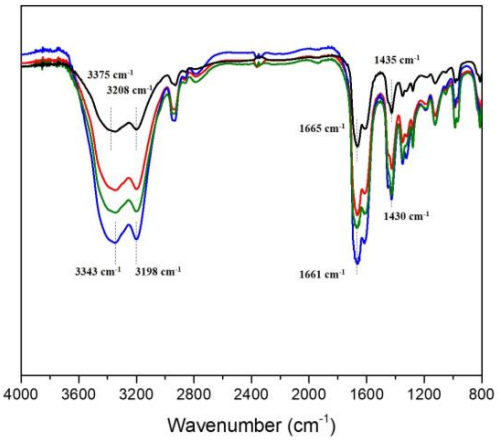

Figure 2. FT-IR spectra of PAID hydrogels. (Black for PAID-0, red for PAID-1, green for PAID-2, and blue for PAID-3).

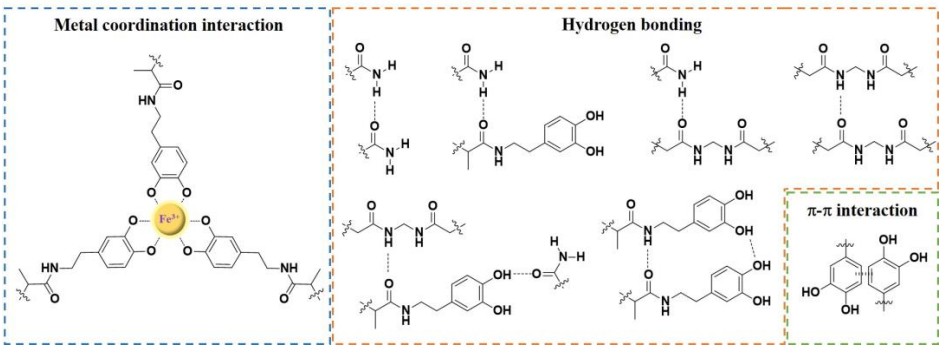

Figure 3. Proposed potential molecular interactions in PAID hydrogels.

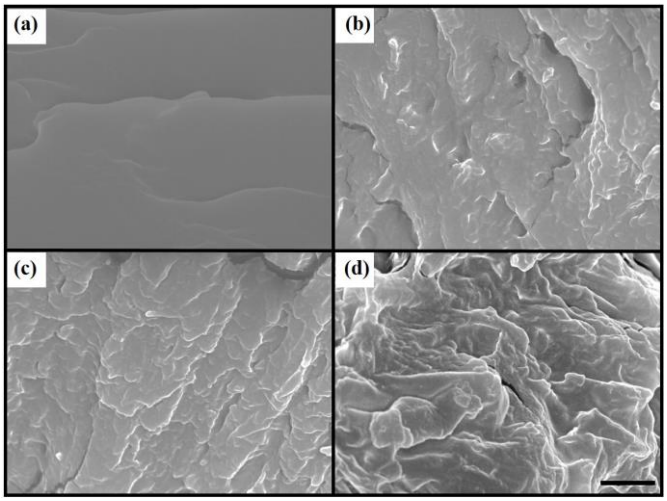

Figure 4. SEM images of (**a**) PAID-0, (**b**) PAID-1, (**c**) PAID-2, and (**d**) PAID-3 hydrogels. (Scale bar: 1 μm).

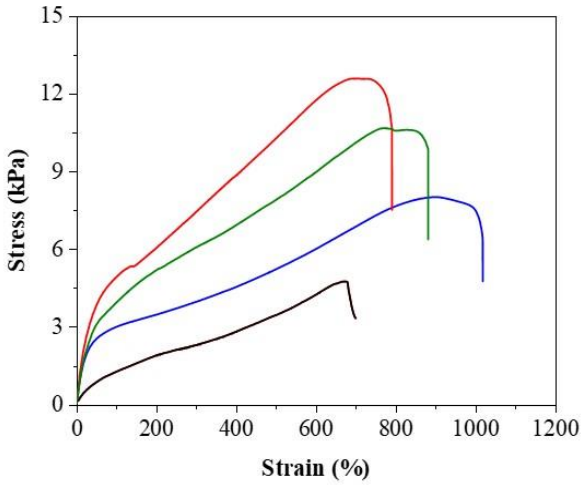

Figure 5. Tensile stress-strain curves of PAID hydrogels. (Black for PAID-0, red for PAID-1, green for PAID-2, and blue for PAID-3).

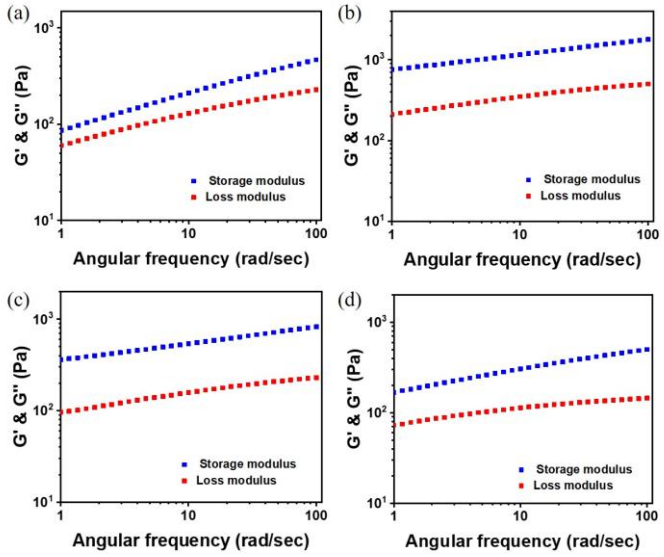

Figure 6. Frequency-dependent (ω = 0.1–100 rad/sec) rheology measurement of (**a**) PAID-0, (**b**) PAID-1, (**c**) PAID-2, and (**d**) PAID-3 hydrogels.

3.4. Biocompatibility of PAID Hydrogels

For biomedical applications, it is crucial to assess the biocompatibility of hydrogels [61–64]. In order to evaluate hydrogels' compatibility with living cells, the widely-used MTT assay was employed [65,66]. This assay provides valuable insights into the viability and metabolic activity of cells in the presence of the hydrogels, aiding in determining their suitability for use in various biomedical applications such as tissue engineering and drug delivery systems. As depicted in Figure 7, the cell viability of L929 cells on PAID hydrogels was assessed for 1, 3, and 7 days. The cell survival rate of L929 cells cultured in these hydrogels for 7 days was above 90%, confirming the exceptional biocompatibility of PAID hydrogels. The statistical analysis of *p*-values was conducted using the Student's *t*-test and is summarized in Table S4. The significance of these *p*-values lies in their capacity to determine whether the differences observed between the groups are statistically meaningful. A *p*-value below the conventional threshold of 0.05 indicates that the observed differences are not likely the result of random chance alone, demonstrating a statistically significant outcome. It is well established that polyacrylamide-based gels can undergo degradation under various environmental conditions, including chemical, photolytic, thermal, mechanical, and biological processes. Among them, the biodegradation characteristics of hydrogels play a crucial role in drug delivery and tissue engineering. Therefore, we evaluated the degradation of PAID hydrogels in a phosphate-buffered saline solution at 37 °C; the results are depicted in Figure S1. The degradation rates of the hydrogels follow the order PAID-0 > PAID-3 ≈ PAID-2 > PAID-1, which correlates with their mechanical strength trends. This indicates that metal-coordination interactions may be the predominant factor driving degradation (Figure S1).

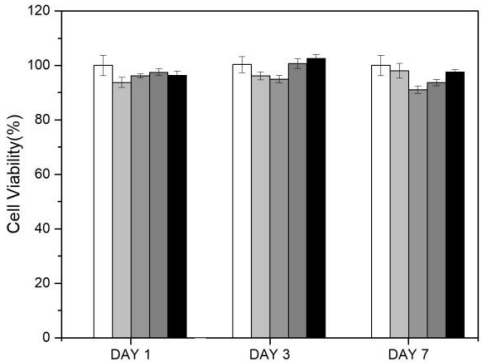

Figure 7. Cell viability of L929 cells on PAID hydrogels for 1, 3, and 7 days. The arrangement from left to right includes the following: control, PAID-0, PAID-1, PAID-2, and PAID-3.

3.5. Adhesive and Stretchable Capacities of PAID Hydrogels

Taking into account both mechanical properties and biocompatibility, we decided to conduct additional adhesion and stretchability tests specifically on the PAID-3 hydrogel [66–68]. Our findings indicate that PAID-3 has good adhesion to glass, plastic, stainless steel, gloves, aluminum, and wood, as demonstrated in Figure 8. Due to the adhesive nature of PAID-3 to various materials, we propose a potential interface adhesion mechanism between PAID-3 and the substrate (Figure 9) [69]. Moreover, we measured the adhesive strength of PAID-3 on various substrates and compared it with the literature (Figure S2 and Table S3). Our results demonstrated that PAID-3 exhibited strong adhesive properties, with an adhesive strength of approximately 15.2 kPa on glass. Furthermore, we employed PAID-3 as an adhesive for glass, as illustrated in Figure 10a. By sandwiching PAID-3 between two glass pieces, we observed its effective adhesion to glass surfaces. Additionally, we applied PAID-3 to the fingers of both hands and conducted tests involving tensile forces and weight support (Figure 10b). Remarkably, PAID-3 exhibited exceptional adhesion to the skin, impressive stretchability, and remarkable weight-bearing capabilities. The excellent adhesiveness of PAID-3 to various materials may be attributed to the hydrogen-bonding interactions

between AMM and the substrate, as well as the hydrogen bonding and metal coordination between DA and the substrate [70,71]. Figure 10c presents the stretch test result of PAID-3, where the initial size of the hydrogel was 1.5 cm and it demonstrated the ability to stretch over 22 times its original length. Finally, we proceeded to verify the elasticity and toughness of PAID-3. For this purpose, we conducted an experiment where a 500 mL water bottle (filled with water) was supported using PAID-3, and the hydrogel/water bottle was subjected to shaking (Video S1). This test confirmed the excellent resilience and toughness of PAID-3. Consequently, we have successfully developed a hydrogel that combines stretchability, adhesion, and biocompatibility through the synergistic effects of utilizing iron–DA complexes, π-π interaction, and the hydrogen-bond force of DA. This achievement not only holds significant potential for biomedical engineering applications but also for corrosion protection, anti-fouling, and more [72–74].

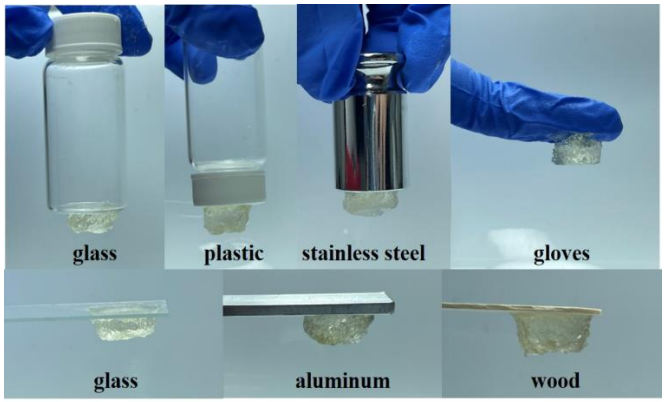

Figure 8. The adhesive properties of the PAID-3 hydrogel were evaluated on various substrates such as glass, plastic, stainless steel, gloves, aluminum, and wood.

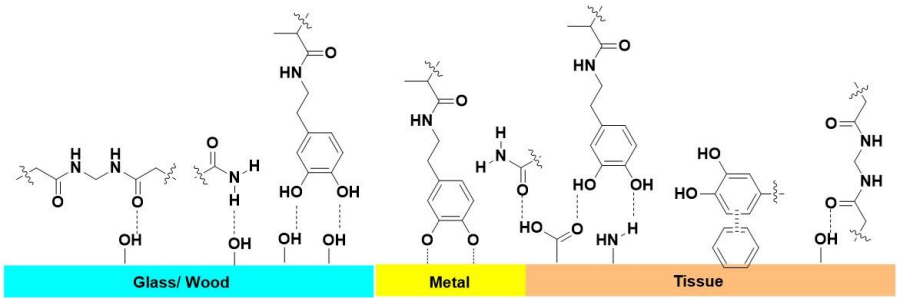

Figure 9. Schematic representation of the interface adhesion mechanism of the PAID-3 hydrogel to various substrates.

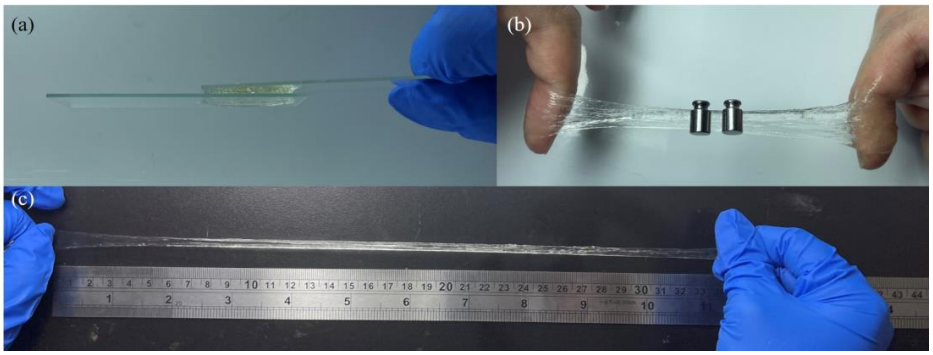

Figure 10. Adhesion, stretchability, and support properties of the PAID-3 hydrogel. (**a**) PAID-3 functions as a glass adhesive, (**b**) PAID-3 adheres to fingers and can successfully support the weight of a weight mass, and (**c**) Stretch testing of PAID-3.

4. Conclusions

In summary, we synthesized four hydrogels incorporating AAM, MBA, and DA and investigated the impact of different ratios of iron (III) ions to DA on each hydrogel's performance. Our research encompassed FT-IR, SEM, tensile stress-strain, and rheology experiments to elucidate the correlation between material properties and intermolecular forces. Through our analysis of PAID-0 and PAID-1, we validated the significance of metal coordination in enhancing the stiffness and toughness of hydrogels. Moreover, by increasing the dopamine content, we achieved improved stretchability and adhesion capabilities in the hydrogels (PAID-1, PAID-2, and PAID-3). Ultimately, we selected the PAID-3 hydrogel with optimal mechanical properties for adhesion testing on various materials. Remarkably, PAID-3 exhibited good adhesion to diverse materials as well as the low cytotoxicity of PAID hydrogel. Overall, it showcased great promise as a new option for biomedical engineering applications.

Supplementary Materials: The following supporting information can be downloaded at: https://www.mdpi.com/article/10.3390/polym15224378/s1. Table S1: Physical properties of PAID hydrogels; Table S2: Comparison of tensile stress-strain performance between this work and previously reported hydrogels; Table S3: Comparison of adhesive strength between this work and previously reported hydrogels; Table S4: Summarized *t*-test table of *p*-values for cell viability; Figure S1: Degradation curves of PAID hydrogels; Figure S2: Lap-shear strength tests of the PAID-3 hydrogel on different substrates; Figure S3: ^{1}H NMR spectrum of methacrylic-modified dopamine in D_2O; Video S1: Testing of the elasticity and toughness of the PAID-3 hydrogel. References [43,48,75–86] are cited in the supplementary materials.

Author Contributions: Conceptualization, M.-Y.Y., H.-C.L. and J.W.; methodology, C.L. and H.-S.H.; validation, C.L., H.-S.H., Y.-Y.W., Y.-S.Z. and R.D.C.; formal analysis, C.L., H.-S.H. and Y.-Y.W.; investigation, C.L. and Y.-S.Z.; resources, writing—original draft preparation, writing—review and editing, supervision, project administration, and funding acquisition, M.-Y.Y., H.-C.L. and J.W. All authors have read and agreed to the published version of the manuscript.

Funding: The study was supported by the National Science and Technology Council of the Republic of China, Taiwan (NSTC 112-2113-M-A49-004, 111-2113-M-A49-030, 111-2923-M-A49-002-MY3, and 112-2113-M-033-003).

Institutional Review Board Statement: Not applicable.

Data Availability Statement: All needed data are in the Article.

Acknowledgments: We gratefully acknowledge support from the National Science and Technology Council of the Republic of China, Taiwan.

Conflicts of Interest: The authors declare no conflict of interest.

References

1. Zhao, X.; Chen, X.; Yuk, H.; Lin, S.; Liu, X.; Parada, G. Soft Materials by Design: Unconventional Polymer Networks Give Extreme Properties. *Chem. Rev.* **2021**, *121*, 4309–4372. [CrossRef] [PubMed]
2. Gong, J.P. Materials both Tough and Soft. *Science* **2014**, *344*, 161–162. [CrossRef] [PubMed]
3. Ahmed, M.M. Hydrogel: Preparation, characterization, and applications: A review. *J. Adv. Res.* **2015**, *6*, 105–121. [CrossRef] [PubMed]
4. Yazdi, M.K.; Vatanpour, V.; Taghizadeh, A.; Taghizadeh, M.; Ganjali, M.R.; Munir, M.T.; Habibzadeh, S.; Saeb, M.R.; Ghaedi, M. Hydrogel membranes: A review. *Mater. Sci. Eng. C* **2020**, *114*, 111023. [CrossRef] [PubMed]
5. Appel, E.A.; Loh, X.J.; Jones, S.T.; Biedermann, F.; Dreiss, C.A.; Scherman, O.A. Ultrahigh-Water-Content Supramolecular Hydrogels Exhibiting Multistimuli Responsiveness. *J. Am. Chem. Soc.* **2012**, *134*, 11767–11773. [CrossRef]
6. Kuang, X.; Arican, M.O.; Zhou, T.; Zhao, X.; Zhang, Y.S. Functional Tough Hydrogels: Design, Processing, and Biomedical Applications. *Acc. Mater. Res.* **2023**, *4*, 101–114. [CrossRef]
7. Wang, Z.; Li, H.; Tang, Z.; Liu, Z.; Ruan, Z.; Ma, L.; Yang, Q.; Wang, D.; Zhi, C. Hydrogel Electrolytes for Flexible Aqueous Energy Storage Devices. *Adv. Funct. Mater.* **2018**, *28*, 1804560. [CrossRef]
8. Ting, M.S.; Travas-Sejdic, J.; Malmström, J. Modulation of hydrogel stiffness by external stimuli: Soft materials for mechanotransduction studies. *J. Mater. Chem. B* **2021**, *9*, 7578–7596. [CrossRef]

9. Huang, J.; Frauenlob, M.; Shibata, Y.; Wang, L.; Nakajima, T.; Nonoyama, T.; Tsuda, M.; Tanaka, S.; Kurokawa, T.; Gong, J.P. Chitin-Based Double-Network Hydrogel as Potential Superficial Soft-Tissue-Repairing Materials. *Biomacromolecules* **2020**, *21*, 4220–4230. [CrossRef]
10. Lee, K.Y.; Mooney, D.J. Hydrogels for Tissue Engineering. *Chem. Rev.* **2001**, *101*, 1869–1880. [CrossRef]
11. Spicer, C.D. Hydrogel scaffolds for tissue engineering: The importance of polymer choice. *Polym. Chem.* **2020**, *11*, 184–219. [CrossRef]
12. Radulescu, D.-M.; Neacsu, I.A.; Grumezescu, A.-M.; Andronescu, E. New Insights of Scaffolds Based on Hydrogels in Tissue Engineering. *Polymers* **2022**, *14*, 799. [CrossRef] [PubMed]
13. Lee, Y.; Song, W.J.; Sun, J.-Y. Hydrogel soft robotics. *Mater. Today Phys.* **2020**, *15*, 100258. [CrossRef]
14. Ouyang, Y.; Huang, G.; Cui, J.; Zhu, H.; Yan, G.; Mei, Y. Advances and Challenges of Hydrogel Materials for Robotic and Sensing Applications. *Chem. Mater.* **2022**, *34*, 9307–9328. [CrossRef]
15. Jing, L.; Hsiao, L.-Y.; Li, S.; Yang, H.; Ng, P.L.P.; Ding, M.; Truong, T.V.; Ga, S.-P.; Li, K.; Guo, Y.-X.; et al. 2D-Material-integrated hydrogels as multifunctional protective skins for soft robots. *Mater. Horiz.* **2021**, *8*, 2065–2078. [CrossRef] [PubMed]
16. Jiang, J.; Xu, S.; Ma, H.; Li, C.; Huang, Z. Photoresponsive hydrogel-based soft robot: A review. *Mater. Today Bio* **2023**, *20*, 100657. [CrossRef] [PubMed]
17. Dong, X.; Luo, X.; Zhao, H.; Qiao, C.; Li, J.; Yi, J.; Yang, L.; Oropeza, F.J.; Hu, T.S.; Xu, Q.; et al. Recent advances in biomimetic soft robotics: Fabrication approaches, driven strategies and applications. *Soft. Matter.* **2022**, *18*, 7699–7734. [CrossRef]
18. Liu, Y.-J.; Cao, W.-T.; Ma, M.-G.; Wan, P. Ultrasensitive Wearable Soft Strain Sensors of Conductive, Self-healing, and Elastic Hydrogels with Synergistic "Soft and Hard" Hybrid Networks. *ACS Appl. Mater. Interfaces* **2017**, *9*, 25559–25570. [CrossRef]
19. Zhang, L.; Wan, C.; Su, J.; Zhang, C.; Wei, S.; Tian, W.; Liu, X.; Cheng, W.; Li, X.; Li, X.; et al. A dual-crosslinked self-healing and antibacterial nanocellulose hydrogel for monitoring of human motions. *Mater. Des.* **2022**, *215*, 110464. [CrossRef]
20. Chen, Z.; Chen, Y.; Hedenqvist, M.S.; Chen, C.; Cai, C.; Li, H.; Liu, H.; Fu, J. Multifunctional conductive hydrogels and their applications as smart wearable devices. *J. Mater. Chem. B* **2021**, *9*, 2561–2583. [CrossRef]
21. Rahmani, P.; Shojaei, A. A review on the features, performance and potential applications of hydrogel-based wearable strain/pressure sensors. *Adv. Colloid Interface Sci.* **2021**, *298*, 102553. [CrossRef] [PubMed]
22. Bashari, A.; Shirvan, A.R.; Shakeri, M. Cellulose-based hydrogels for personal care products. *Polym. Adv. Technol.* **2018**, *29*, 2853–2867. [CrossRef]
23. Zhang, A.; Liu, Y.; Qin, D.; Sun, M.; Wang, T.; Chen, X. Research status of self-healing hydrogel for wound management: A review. *Int. J. Biol. Macromol.* **2020**, *164*, 2108–2123. [CrossRef] [PubMed]
24. Mitura, S.; Sionkowska, A.; Jaiswal, A. Biopolymers for hydrogels in cosmetics: Review. *J. Mater. Sci. Mater. Med.* **2020**, *31*, 50. [CrossRef]
25. Xue, K.; Liow, S.S.; Karim, A.A.; Li, Z.; Loh, X.J. A Recent Perspective on Noncovalently Formed Polymeric Hydrogels. *Chem. Rec.* **2018**, *18*, 1517–1529. [CrossRef]
26. Xu, K.; Shen, K.; Yu, J.; Yang, Y.; Wei, Y.; Lin, P.; Zhang, Q.; Xiao, C.; Zhang, Y.; Cheng, Y. Ultradurable Noncovalent Cross-Linked Hydrogels with Low Hysteresis and Robust Elasticity for Flexible Electronics. *Chem. Mater.* **2022**, *34*, 3311–3322. [CrossRef]
27. Panzer, M.J. Holding it together: Noncovalent cross-linking strategies for ionogels and eutectogels. *Mater. Adv.* **2022**, *3*, 7709–7725. [CrossRef]
28. Panja, S.; Seddon, A.; Adams, D.J. Controlling hydrogel properties by tuning non-covalent interactions in a charge complementary multicomponent system. *Chem. Sci.* **2021**, *12*, 11197–11203. [CrossRef]
29. Wang, W.; Zhang, Y.; Liu, W. Bioinspired fabrication of high strength hydrogels from non-covalent interactions. *Prog. Polym. Sci.* **2017**, *71*, 1–25. [CrossRef]
30. Zhang, M.; Yu, J.; Shen, K.; Wang, R.; Du, J.; Zhao, X.; Yang, Y.; Xu, K.; Zhang, Q.; Zhang, Y.; et al. Highly Stretchable Nanocomposite Hydrogels with Outstanding Antifatigue Fracture Based on Robust Noncovalent Interactions for Wound Healing. *Chem. Mater.* **2021**, *33*, 6453–6463. [CrossRef]
31. Yu, A.C.; Lian, H.; Kong, X.; Hernandez, H.L.; Qin, J.; Appel, E.A. Physical networks from entropy-driven non-covalent interactions. *Nat. Commun.* **2021**, *12*, 746. [CrossRef] [PubMed]
32. Pinnataip, R.; Lee, B.P. Oxidation Chemistry of Catechol Utilized in Designing Stimuli-Responsive Adhesives and Antipathogenic Biomaterials. *ACS Omega* **2021**, *6*, 5113–5118. [CrossRef] [PubMed]
33. Guo, Q.; Chen, J.; Wang, J.; Zeng, H.; Yu, J. Recent progress in synthesis and application of mussel-inspired adhesives. *Nanoscale* **2020**, *12*, 1307–1324. [CrossRef] [PubMed]
34. Kim, B.J.; Kim, S.; Oh, D.X.; Masic, A.; Cha, H.J.; Hwang, D.S. Mussel-inspired adhesive protein-based electrospun nanofibers reinforced by Fe(iii)–DOPA complexation. *J. Mater. Chem. B* **2015**, *3*, 112–118. [CrossRef]
35. Li, L.; Smitthipong, W.; Zeng, H. Mussel-inspired hydrogels for biomedical and environmental applications. *Polym. Chem.* **2015**, *6*, 353–358. [CrossRef]
36. Li, X.; Qiu, H.; Gao, P.; Yang, Y.; Yang, Z.; Huang, N. Synergetic coordination and catecholamine chemistry for catalytic generation of nitric oxide on vascular stents. *NPG Asia Mater.* **2018**, *10*, 482–496. [CrossRef]
37. Li, Y.; Cao, Y. The molecular mechanisms underlying mussel adhesion. *Nanoscale Adv.* **2019**, *1*, 4246–4257. [CrossRef]

38. Dutta, A.; Ghosal, K.; Sarkar, K.; Pradhan, D.; Das, R.K. From ultrastiff to soft materials: Exploiting dynamic metal–ligand cross-links to access polymer hydrogels combining customized mechanical performance and tailorable functions by controlling hydrogel mechanics. *Chem. Eng. J.* **2021**, *419*, 129528. [CrossRef]
39. Guo, Y.; Gao, Z.; Liu, Y.; Huang, Z.; Chai, C.; Hao, J. Multiple Cross-Linking-Dominated Metal–Ligand Coordinated Hydrogels with Tunable Strength and Thermosensitivity. *ACS Appl. Polym. Mater.* **2019**, *1*, 2370–2378. [CrossRef]
40. Gan, F.; Wang, J.; Wen, J.; Zhou, J.; Mo, J.; Han, S.; Wu, Y.; Yi, N. Preparation of polyimide-metal complexes with tunable Sol-Gel transition by Introduction of Zn(II)-Coordination. *Polym. Test.* **2022**, *111*, 107615. [CrossRef]
41. Sun, W.; Xue, B.; Fan, Q.; Tao, R.; Wang, C.; Wang, X.; Li, Y.; Qin, M.; Wang, W.; Chen, B.; et al. Molecular engineering of metal coordination interactions for strong, tough, and fast-recovery hydrogels. *Sci. Adv.* **2020**, *6*, 9531. [CrossRef] [PubMed]
42. Zheng, S.Y.; Ding, H.; Qian, J.; Yin, J.; Wu, Z.L.; Song, Y.; Zheng, Q. Metal-Coordination Complexes Mediated Physical Hydrogels with High Toughness, Stick–Slip Tearing Behavior, and Good Processability. *Macromolecules* **2016**, *49*, 9637–9646. [CrossRef]
43. Ju, H.; Zhu, Q.L.; Zuo, M.; Liang, S.; Du, M.; Zheng, Q.; Wu, Z.L. Toughening Hydrogels by Forming Robust Hydrazide-Transition Metal Coordination Complexes. *Chem. Eur. J.* **2023**, *29*, e202300969. [CrossRef] [PubMed]
44. Holten-Andersen, N.; Harrington, M.J.; Birkedal, H.; Lee, B.P.; Messersmith, P.B.; Lee, K.Y.C.; Waite, J.H. pH-induced metal-ligand cross-links inspired by mussel yield self-healing polymer networks with near-covalent elastic moduli. *Proc. Natl. Acad. Sci. USA* **2011**, *108*, 2651–2655. [CrossRef] [PubMed]
45. Vehlow, D.; Wong, J.P.H.; Urban, B.; Weisspflog, J.; Gebert, A.; Schumacher, M.; Gelinsky, M.; Stamm, M.; Muller, M. Catechol Containing Polyelectrolyte Complex Nanoparticles as Local Drug Delivery System for Bortezomib at Bone Substitute Materials. *Pharmaceutics* **2020**, *12*, 799. [CrossRef]
46. Su, J.; Chen, F.; Cryns, V.L.; Messersmith, P.B. Catechol polymers for pH-responsive, targeted drug delivery to cancer cells. *J. Am. Chem. Soc.* **2011**, *133*, 11850–11853. [CrossRef]
47. Chandra Joshi, D.; Ashokan, A.; Jayakannan, M. l-Amino Acid Based Phenol- and Catechol-Functionalized Poly(ester-urethane)s for Aromatic pi-Interaction Driven Drug Stabilization and Their Enzyme-Responsive Delivery in Cancer Cells. *ACS Appl. Bio Mater.* **2022**, *5*, 5432–5444. [CrossRef]
48. Glass, P.; Chung, H.; Washburn, N.R.; Sitti, M. Enhanced Reversible Adhesion of Dopamine Methacrylamide-Coated Elastomer Microfibrillar Structures under Wet Conditions. *Langmuir* **2009**, *25*, 6607–6612. [CrossRef]
49. Zheng, Y.; Liang, Y.; Zhang, D.; Sun, X.; Liang, L.; Li, J.; Liu, Y.-N. Gelatin-Based Hydrogels Blended with Gellan as an Injectable Wound Dressing. *ACS Omega* **2018**, *3*, 4766–4775. [CrossRef]
50. Zangmeister, R.A.; Morris, T.A.; Tarlov, M.J. Characterization of Polydopamine Thin Films Deposited at Short Times by Autoxidation of Dopamine. *Langmuir* **2013**, *29*, 8619–8628. [CrossRef]
51. Schäfer, S.; Kickelbick, G. Double Reversible Networks: Improvement of Self-Healing in Hybrid Materials via Combination of Diels–Alder Cross-Linking and Hydrogen Bonds. *Macromolecules* **2018**, *51*, 6099–6110. [CrossRef]
52. Hsu, S.-M.; Lin, Y.-C.; Chang, J.-W.; Liu, Y.-H.; Lin, H.-C. Intramolecular Interactions of a Phenyl/Perfluorophenyl Pair in the Formation of Supramolecular Nanofibers and Hydrogels. *Angew. Chem. Int. Ed.* **2014**, *53*, 1921–1927. [CrossRef] [PubMed]
53. Chen, P.-W.; Ji, D.-H.; Zhang, Y.-S.; Lee, C.; Yeh, M.-Y. Electroactive and Stretchable Hydrogels of 3,4-Ethylenedioxythiophene/thiophene Copolymers. *ACS Omega* **2023**, *8*, 6753–6761. [CrossRef]
54. Yildiz, G.; Çatalgil-Giz, H.; Kadirgan, F. Electrochemically prepared acrylamide/N,N′-methylene bisacrylamide gels. *J. Appl. Electrochem.* **2000**, *30*, 71–75. [CrossRef]
55. Feng, L.; Zheng, H.; Gao, B.; Zhang, S.; Zhao, C.; Zhou, Y.; Xu, B. Fabricating an anionic polyacrylamide (APAM) with an anionic block structure for high turbidity water separation and purification. *RSC Adv.* **2017**, *7*, 28918–28930. [CrossRef]
56. Wang, J.; Lin, Y.; Mohamed, A.; Ji, Q.; Jia, H. High strength and flexible aramid nanofiber conductive hydrogels for wearable strain sensors. *J. Mater. Chem. C* **2021**, *9*, 575–583. [CrossRef]
57. Lv, Z.; Liu, J.; Yang, X.; Fan, D.; Cao, J.; Luo, Y.; Zhang, X. Naturally Derived Wearable Strain Sensors with Enhanced Mechanical Properties and High Sensitivity. *ACS Appl. Mater. Interfaces* **2020**, *12*, 22163–22169. [CrossRef]
58. Ramli, H.; Zainal, N.F.A.; Hess, M.; Chan, C.H. Basic principle and good practices of rheology for polymers for teachers and beginners. *Chem. Teach. Int.* **2022**, *4*, 307–326. [CrossRef]
59. Stojkov, G.; Niyazov, Z.; Picchioni, F.; Bose, R.K. Relationship between Structure and Rheology of Hydrogels for Various Applications. *Gels* **2021**, *7*, 255. [CrossRef]
60. Yan, C.; Pochan, D.J. Rheological properties of peptide-based hydrogels for biomedical and other applications. *Chem. Soc. Rev.* **2010**, *39*, 3528–3540. [CrossRef]
61. Pilipenko, I.; Murzova, A.; Savin, A.; Mohamed, A.A.; Vladimirova, E.; Koshel, E.; Shamova, O.; Kumacheva, E. Dual-Function Hydrogel Dressings with a Dynamic Exchange of Iron Ions and an Antibiotic Drug for Treatment of Infected Wounds. *ACS Appl. Bio Mater.* **2023**, *6*, 1896–1905. [CrossRef] [PubMed]
62. Li, Y.; Yang, K.; Wang, Z.; Xiao, J.; Tang, Z.; Li, H.; Yi, W.; Li, Z.; Luo, Y.; Li, J.; et al. Rapid In Situ Deposition of Iron-Chelated Polydopamine Coating on the Polyacrylamide Hydrogel Dressings for Combined Photothermal and Chemodynamic Therapy of Skin Wound Infection. *ACS Appl. Bio Mater.* **2022**, *5*, 4541–4553. [CrossRef] [PubMed]
63. Zheng, X.; Wu, H.; Wang, S.; Zhao, J.; Hu, L. Preparation and Characterization of Biocompatible Iron/Zirconium/Polydopamine/Carboxymethyl Chitosan Hydrogel with Fenton Catalytic Properties and Photothermal Efficacy. *Gels* **2023**, *9*, 452. [CrossRef] [PubMed]

64. Kim, J.Y.; Ryu, S.B.; Park, K.D. Preparation and characterization of dual-crosslinked gelatin hydrogel via Dopa-Fe^{3+} complexation and fenton reaction. *J. Ind. Eng. Chem.* **2018**, *58*, 105–112. [CrossRef]
65. Barltrop, J.A.; Owen, T.C.; Cory, A.H.; Gory, J.G. 5-(3-carboxymethoxyphenyl)-2-(4,5-dimethylthiazolyl)-3-(4-sulfophenyl)tetrazolium, inner salt (MTS) and related analogs of 3-(4,5-dimethylthiazolyl)-2,5-diphenyltetrazolium bromide (MTT) reducing to purple water-soluble formazans As cell-viability indicators. *Bioorganic Med. Chem. Lett.* **1991**, *1*, 611–614.
66. Yeh, M.-Y.; Zhao, J.-Y.; Hsieh, Y.-R.; Lin, J.-H.; Chen, F.-Y.; Chakravarthy, R.D.; Chung, P.-C.; Lin, H.-C.; Hung, S.-C. Reverse thermo-responsive hydrogels prepared from Pluronic F127 and gelatin composite materials. *RSC Adv.* **2017**, *7*, 21252–21257. [CrossRef]
67. Bovone, G.; Dudaryeva, O.Y.; Marco-Dufort, B.; Tidditt, M.W. Engineering Hydrogel Adhesion for Biomedical Applications via Chemical Design of the Junction. *ACS Biomater. Sci. Eng.* **2021**, *7*, 4048–4076. [CrossRef]
68. Guo, M.; Li, G.; Cai, M.; Hou, X.; Huang, K.; Tang, J.; Guo, C.F. A Tough Hydrogel Adhesive for the Repair of Archeological Pottery. *Nano Lett.* **2023**, *23*, 1371–1378. [CrossRef]
69. Zhang, W.; Wang, R.; Sun, Z.; Zhu, X.; Zhao, Q.; Zhang, T.; Cholewinski, A.; Yang, F.K.; Zhao, B.; Pinnaratip, R.; et al. Catechol-functionalized hydrogels: Biomimetic design, adhesion mechanism, and biomedical applications. *Chem. Soc. Rev.* **2020**, *49*, 433–464. [CrossRef]
70. Fan, X.; Wang, S.; Fang, Y.; Li, P.; Zhou, W.; Wang, Z.; Chen, M.; Liu, H. Tough polyacrylamide-tannic acid-kaolin adhesive hydrogels for quick hemostatic application. *Mater. Sci. Eng. C* **2020**, *109*, 110649. [CrossRef]
71. Xu, Z.; Chen, L.; Lu, L.; Du, R.; Ma, W.; Cai, Y.; An, X.; Wu, H.; Luo, Q.; Xu, Q.; et al. A Highly-Adhesive and Self-Healing Elastomer for Bio-Interfacial Electrode. *Adv. Funct. Mater.* **2021**, *31*, 2006432. [CrossRef]
72. Ivarsson, M.; Prenkert, M.; Cheema, A.; Wretenberg, P.; Andjelkov, N. Mussel Adhesive Protein as a Promising Alternative to Fibrin for Scaffold Fixation during Cartilage Repair Surgery. *Cartilage* **2021**, *13*, 663S–671S. [CrossRef] [PubMed]
73. Zhang, F.; Chen, C.; Hou, R.; Li, J.; Cao, Y.; Dong, S.; Lin, C.; Pan, J. Investigation and application of mussel adhesive protein nanocomposite film-forming inhibitor for reinforced concrete engineering. *Corros. Sci.* **2019**, *153*, 333–340. [CrossRef]
74. Li, S.; Chen, J.; Wang, J.; Zeng, H. Anti-biofouling materials and surfaces based on mussel-inspired chemistry. *Mater. Adv.* **2021**, *2*, 2216–2230. [CrossRef]
75. Guo, G.; Sun, J.; Wu, Y.; Wang, J.; Zou, L.Y.; Huang, J.J.; Ren, K.F.; Liu, C.M.; Wu, Z.L.; Zheng, Q.; et al. Tough complex hydrogels transformed from highly swollen polyelectrolyte hydrogels based on Cu^{2+} coordination with anti-bacterial properties. *J. Mater. Chem. B* **2022**, *10*, 6414–6424. [CrossRef]
76. Dou, X.; Wang, H.; Yang, F.; Shen, H.; Wang, X.; Wu, D. One-Step Soaking Strategy toward Anti-Swelling Hydrogels with a Stiff "Armor". *Adv. Sci.* **2023**, *10*, e2206242. [CrossRef]
77. Zhang, Y.; Wang, R.; Lu, W.; Li, W.; Chen, S.; Chen, T. Mechanical tough and multicolor aggregation-induced emissive polymeric hydrogels for fluorescent patterning. *Nanoscale Adv.* **2023**, *5*, 725–732. [CrossRef]
78. Zhang, H.; He, J.; Qu, J. High-strength, tough, and anti-swelling Schiff base hydrogels with fluorescent encryption writing, solvent response and double shape memory functions. *Eur. Polym. J.* **2022**, *178*, 111487. [CrossRef]
79. Wei, Z.; Wang, Y.; Cai, C.; Zhang, Y.; Guo, S.; Fu, Y.; Tan, S.C. Dual-Network Liquid Metal Hydrogel with Integrated Solar-Driven Evaporation, Multi-Sensory Applications, and Electricity Generation via Enhanced Light Absorption and Bénard–Marangoni Effect. *Adv. Funct. Mater.* **2022**, *32*, 2206287. [CrossRef]
80. Zhang, Q.; Liu, X.; Duan, L.; Gao, G. Ultra-stretchable wearable strain sensors based on skin-inspired adhesive, tough and conductive hydrogels. *Chem. Eng. J.* **2019**, *365*, 10–19. [CrossRef]
81. Dong, L.; Wang, M.; Wu, J.; Zhu, C.; Shi, J.; Morikawa, H. Stretchable, Adhesive, Self-Healable, and Conductive Hydrogel-Based Deformable Triboelectric Nanogenerator for Energy Harvesting and Human Motion Sensing. *ACS Appl. Mater. Interfaces* **2022**, *14*, 9126–9137. [CrossRef] [PubMed]
82. Chen, T.; Chen, Y.; Rehman, H.U.; Chen, Z.; Yang, Z.; Wang, M.; Li, H.; Liu, H. Ultratough, Self-Healing, and Tissue-Adhesive Hydrogel for Wound Dressing. *ACS Appl. Mater. Interfaces* **2018**, *10*, 33523–33531. [CrossRef] [PubMed]
83. Liao, M.; Wan, P.; Wen, J.; Gong, M.; Wu, X.; Wang, Y.; Shi, R.; Zhang, L. Wearable, Healable, and Adhesive Epidermal Sensors Assembled from Mussel-Inspired Conductive Hybrid Hydrogel Framework. *Adv. Funct. Mater.* **2017**, *27*, 1703852. [CrossRef]
84. Peng, X.; Wang, W.; Yang, W.; Chen, J.; Peng, Q.; Wang, T.; Yang, D.; Wang, J.; Zhang, H.; Zeng, H. Stretchable, compressible, and conductive hydrogel for sensitive wearable soft sensors. *J. Colloid Interface Sci.* **2022**, *618*, 111–120. [CrossRef]
85. Fu, Q.; Hao, S.; Meng, L.; Xu, F.; Yang, J. Engineering Self-Adhesive Polyzwitterionic Hydrogel Electrolytes for Flexible Zinc-Ion Hybrid Capacitors with Superior Low-Temperature Adaptability. *ACS Nano* **2021**, *15*, 18469–18482. [CrossRef]
86. Wang, L.; Zhou, M.; Xu, T.; Zhang, X. Multifunctional hydrogel as wound dressing for intelligent wound monitoring. *Chem. Eng. J.* **2022**, *433*, 134625. [CrossRef]

Disclaimer/Publisher's Note: The statements, opinions and data contained in all publications are solely those of the individual author(s) and contributor(s) and not of MDPI and/or the editor(s). MDPI and/or the editor(s) disclaim responsibility for any injury to people or property resulting from any ideas, methods, instructions or products referred to in the content.